Desalination and Water Treatment
www.deswater.com

doi: 10.5004/dwt.2021.26576

210 (2021) 446–460
January

Adsorption characteristics of *Sauropus androgynus* and its base modified form toward cationic crystal violet dye

Cyndy W.S. Chieng[a], Nur Afiqah Hazirah Mohamad Zaidi[a], Namal Priyantha[b,c], YieChen Lu[a], Linda B.L. Lim[a,*]

[a]*Chemical Sciences Programme, Faculty of Science, Universiti Brunei Darussalam, Gadong, Negara Brunei Darussalam, Tel. 00-673-8748010; emails: linda.lim@ubd.edu.bn (L.B.L. Lim), ccws2206@gmail.com (C.W.S. Chieng), afhazirah@gmail.com (N.A.H. Mohamad Zaidi), yiechen_93@hotmail.com (Y.C. Lu)*
[b]*Department of Chemistry, Faculty of Science, University of Peradeniya, Peradeniya, Sri Lanka, email: namal.priyantha@yahoo.com (N. Priyantha)*
[c]*Postgraduate Institute of Science, University of Peradeniya, Peradeniya, Sri Lanka*

Received 15 April 2020; Accepted 9 September 2020

ABSTRACT

Waste parts of the plant *Sauropus androgynus* (SA), an agricultural by-product, and its base-modified form (MSA) have shown potential for the removal of the cationic crystal violet (CV) dye from aqueous solution. The optimum contact time of SA and MSA was found to be 180 and 120 min, respectively, and no changes in the pH of the system were necessary for optimum performance. SA performed well in moderate ionic environments; and MSA tolerated up to 1.0 M ionic strength. The adsorption process was exothermic. The Sips isotherm model is suitable to describe adsorption of CV on both SA and MSA giving adsorption capacities of 326.38 and 489.58 mg g^{-1}, respectively. Regeneration studies showed that acid and base washings of SA and MSA could regenerate the adsorbents and allowed them to be reused. Given the excellent adsorption capacities, stability at different pH and salt concentrations, ability to be regenerated and reused, both SA and MSA would be deemed suitable new, potential low-cost adsorbents to remove the CV dye in wastewater treatment. More importantly, MSA has demonstrated its superior characteristics to be used in real-life situation for removal of CV dye when present in high ionic environments.

Keywords: Sauropus angrogynus; *Cangkuk manis*; Adsorption isotherm; Crystal violet dye; Regeneration

1. Introduction

Water quality has been affected greatly due to the discharge of pollutants from industrial activities. In textile industry, it is estimated about 12% dyes used in the dyeing process will be lost and discharged as industrial effluents into the environment. Synthetic dyes, being stable and non-biodegradable in nature, lead to their accumulation over long periods of time. Dyes when enter into the water system lower the concentration of dissolved oxygen, thereby affecting the photosynthetic activity of aquatic plants. Further, some dyes have been proven to be carcinogenic and mutagenic to bio-organisms due to the presence of aromatic rings in their structures. Such dyes would cause adverse effects on human health, such as allergies, diarrhea, hyperventilation, skin infection or even immune-suppression, respiratory disorder, central nervous disorder and neurobehavioral disorders on human beings [1–3].

Crystal violet (CV) is a cationic dye that is often used in different industries, such as textiles, cosmetics, paints, papers, and also in medical community [4]. It exists as a

* Corresponding author.

green crystalline solid, but gives a dark purple color solution in water. It is also known as gentian violet or methyl violet 10B due to the presence of six methyl groups in the structure, as shown in Fig. 1. However, despite its uses, CV has been known to pose some threats to human and animals, such as glans penis necrosis, ototoxicity, carcinogenic, and can produce weak mutagenic activity in mammalian cells [5–7]. Owing to its multiple uses such as in biological staining and as a colorant in industries, wastewater effluents which are discharged without pre-treatment may contain CV residues. Thus, it is imperative that CV be removed from wastewater as it is considered a bio-hazardous compound which can affect aquatic life and cause adverse health effects in human [8,9]. Therefore, CV was chosen as the model dye in this study.

Contamination of wastewater is harmful to any form of bio-organisms as it is able to accumulate and pass onto other organisms in the food chain or even through physical contacts. Therefore, environmental concerns and regulations have been raised to minimize and control the amount of pollutants and contaminants being released into any forms of water sources. Treatment of wastewater has been done to clean and remove the pollutants and contaminants present in the water sources. Among the different types of wastewater treatment [10–16], a commonly used method to remove dyes from wastewater is adsorption where pollutants (adsorbates) present in the wastewater get adsorbed onto the surface of the solid phase (adsorbent) [17]. This technique is economically feasible and efficient in the separation of adsorbate from the wastewater. The adsorption process can be either physisorption or chemisorption, depending on the forces and interactions between the adsorbent and adsorbate. The last decade has seen the emergence of various different types of adsorbents, both synthetic and natural, being used to remove heavy metals [18–23] and dyes [24–31]. Not all adsorbents have the ability to remove adsorbates efficiently [32–37], and therefore, the search for an efficient, low-cost adsorbent with high adsorption capacity for a particular adsorbate is still a challenge.

In this study, a new low-cost organic adsorbent is obtained from the waste of a plant named *Sauropus androgynous* (SA), as shown in Fig. 2a. SA, more commonly known as "*Cangkuk manis*," is grown mostly in South Asia, Southeast Asia, and China. It has been widely used in traditional medicine to increase breast milk production, healing of injuries, relieving fever, and urinary disorders and as cure of diabetes [38]. Despite its uses and high nutritional value, excessive intake of SA can cause drowsiness and constipation [39,40]. Consumption of SA over a period can lead to the development of SA-associated obliterative bronchiolitis [41]. In Brunei Darussalam, SA is a popular vegetable often served either fried or as a soup dish. Only the leaves are edible while the stems are thrown away and are of no economical value. Thus, it was decided to make use of the discarded stems and turn them into a potentially useful low-cost adsorbent. To date, there has been no report on the use of SA as an adsorbent in removing pollutants. Hence, this will be the first report on utilizing SA in adsorption study.

The aims of this research are therefore to investigate the suitability of utilizing SA as a low-cost adsorbent to remove CV dye and the possibility of enhancing its removal ability through base modification with sodium hydroxide (NaOH). Studies have shown that base modification is a simple, straightforward, and yet highly efficient method of enhancing adsorption efficiency of an adsorbent. For example, reports have shown that NaOH treatment of rock melon skin showed a 200% increase toward methyl violet 2B dye [42], while *Artocarpus odoratissimus* leaves enhanced its adsorption toward methyl violet 2B and malachite green dyes by approximately 66% and 620%, respectively [43,44]. Therefore, in this study, SA will be chemically modified with NaOH in an attempt to enhance its adsorption toward CV. Characterization using scanning electron microscopy (SEM), Fourier-transform infrared (FTIR) spectroscopy, and point of zero charge (pH_{pzc}) of both SA and its base modified form (MSA) were performed. In addition, effects of various parameters, such as contact time, medium pH, and ionic strength on the extent of adsorption of CV dye by both SA and MSA were studied. Adsorption isotherms and kinetics of both adsorbents toward CV dye were also investigated. Lastly, the dye loaded adsorbents were tested for their regeneration and reusability.

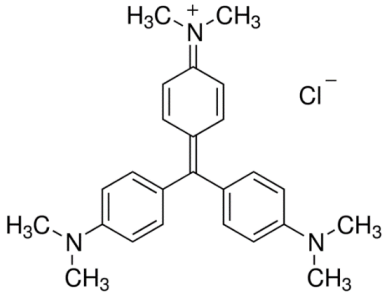

Fig. 1. Chemical structure of CV.

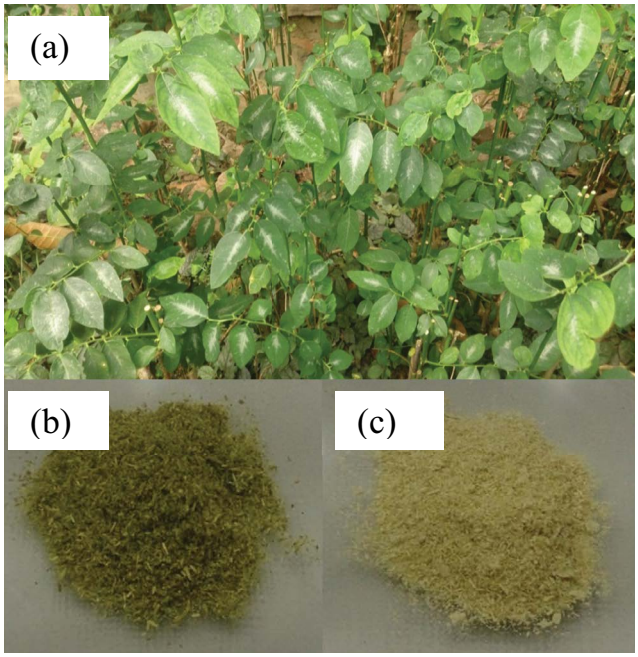

Fig. 2. (a) *Sauropus angrogynus* (SA) plant, (b) Dried SA, and (c) NaOH modified SA (MSA).

2. Methods and materials

2.1. Instrumentation

Meter balance (Precisa Executive Series 360 ES Balance, China) was used to record the masses of samples. The pH of solutions was measured with the EDT directION GP 353 ATC pH meter (UK). Automated shaker (Thermo Scientific MaxQ Shaker, USA), orbital shaker (Stuart SSL1, UK), and flask shaker (Stuart SF1, UK) were used to shake the flasks at 250 rpm containing the adsorbate-adsorbent mixtures. Absorbance of CV dye, before and after adsorption, was measured using UV-vis spectrophotometer (Thermo Scientific Genesys 20, USA). JSM-7610F field emission scanning electron microscopy (FESEM), Japan, was used to observe the surface topography of the adsorbents. FTIR spectrometer (Agilent Technologies Inc., Cary 630 FTIR, USA) was used to obtain the IR spectra in the range of 4,000 and 650 cm^{-1} for the determination of the functional groups present in the adsorbents.

2.2. Chemicals and reagents

Crystal violet (CV) dye, purchased from Sigma-Aldrich (USA) with molecular formula $C_{25}H_{30}ClN_3$ (molar mass 407.99 g mol^{-1}), was used as the adsorbate to be removed in this research. NaOH, purchased from Merck (USA), was used to modify SA and also as the washing reagent in regeneration study. Sodium chloride (NaCl) and sodium nitrate ($NaNO_3$) were purchased from Sigma-Aldrich, while hydrochloric acid (HCl), potassium chloride (KCl) and potassium nitrate (KNO_3) were from Merck. All chemicals and reagents were used without further purification.

2.3. Preparation of SA and its surface modification

The *Sauropus angrogynus* (SA) plants were purchased from a local supermarket in the Brunei-Muara District, in Brunei Darussalam. The stems, being the inedible parts of the plant which are thrown away, were collected and cut into small pieces, washed throughout using double distilled water until free of dirt and dust. The washed sample was then dried in an oven at 60°C until a constant mass was obtained in order to assure that all the water in the sample has been removed. Dried sample was then blended and sieved using a set of laboratory sieves to obtain particles of diameter <355 μm (Fig. 2b).

SA was modified by shaking the sample in 1 M NaOH for 120 min. The modified SA (MSA) was filtered and washed with distilled water until the pH was approximately at 7. Lastly, the MSA was dried in an oven at 60°C. The dried MSA, as shown in Fig. 2c, was kept in a dry, clean and well-sealed zip lock bag until ready to be used.

2.4. Point of zero charge

Point of zero charge (pH_{PZC}) was carried out to investigate the pH when the electrical charge on the adsorbent's surface is zero, following the procedure as outlined by Zehra et al. [45]. A mass of 0.050 g of the adsorbent was shaken in 25.0 mL of 0.1 M of KNO_3 with the pH adjusted to 2, 4, 6, 8, and 10 for period of 24 h. No adsorbate was used in the experiment.

2.5. Optimization of adsorption parameters

Optimization of parameters for contact time (0–240 min), medium pH (2–12), and ionic strength using four salts (NaCl, KCl, $NaNO_3$, and KNO_3) at different concentrations (0, 0.01, 0.1, 0.2, 0.4, 0.6, 0.8, and 1.0 M) were carried out prior to performing adsorption isotherm and kinetics studies. All adsorption experiments were done using mixtures of 0.05 g of adsorbent in 25.0 mL of dye at specified concentration (adsorbent:adsorbate ratio is 1 g:500 mL), and the mixture was shaken on an orbital shaker set at 250 rpm. At the end of all adsorption experiments, each mixture was filtered through a metal sieve and the filtrates were collected and diluted, if necessary, before their absorbance was measured. The initial and final absorbance values of the dye were used to determine the extent of dye removal. All experiments were carried out in duplicate, unless otherwise stated, to obtain an average result. The adsorption capacity (q_e), expressed in mg of dye adsorbed by per of adsorbent (mg g^{-1}), can be calculated by using Eq. (1):

$$q_e = \frac{(C_0 - C_e)V}{m} \tag{1}$$

where C_0 is the initial concentration of adsorbate in mg L^{-1}, C_e is the final concentration of adsorbate in mg L^{-1}, V is the volume of adsorbate used in L, and m is the mass of adsorbate used in g.

The percentage removal (%) of adsorbate in the system can then be calculated using Eq. (2):

$$\%\ \text{removal} = \frac{(C_0 - C_e)}{C_o} \times 100 \tag{2}$$

2.6. Batch adsorption experiments

Batch adsorption isotherm experiments of CV by SA and MSA were carried out by shaking the absorbent with various concentrations of the dye ranging from 0 to 1,000 mg L^{-1} at ambient temperature (25°C) for its optimum shaking time. To investigate the effect of temperature on adsorption, the experiments were carried out by shaking adsorbent-CV mixture at 298, 313, 323, 333, and 343 K at the optimum contact time in a thermostatic water bath.

2.7. Regeneration study

Regeneration study was carried out following the methods outlined by Dahri et al. [46] with slight modification. Briefly, a sample of 1.00 g each of SA and MSA was separately agitated with 500 mL of 800 mg L^{-1} CV dye according to their optimum contact time to obtain adsorbents saturated with CV dyes. Desorption studies were subsequently carried out by dividing the dye saturated samples into five portions. Three portions were shaken with different solutions: 0.1 M of HCl, 0.1 M of NaOH and distilled water, whereas another portion was quick washed with distilled

water and a control of the experiment was also included for comparison. In the desorption study, the ratio of mass of adsorbent (g) to washing solution (mL) was kept at 1:50.

3. Results and discussion

3.1. Characterization of adsorbents

SEM images in Fig. 3 show SA and MSA before and after adsorption of CV dye. Prior to surface modification, the majority of the surface of SA is generally flat and smooth, even though there are some folds and pores. In contrast, base modification drastically altered the surface morphology of SA. The surface of MSA became more undulating with the formation of more deep pores or holes, causing the surface to be rougher and more exposed. This increases the surface area and active sites present on the adsorbent's surface. After adsorption of CV by SA and MSA, pores, and active sites on the surface of both the adsorbents were seen to be covered by the CV dye.

The FTIR spectrum of SA identifies a few functional groups: the broad band at 3,263 cm^{-1} indicates the presence of hydroxyl group (–OH), weak band at 2,913 cm^{-1} indicates that (C–H) bond in methyl group ($–CH_3$) is present, a medium stretching band at 1,617 cm^{-1} confirms the presence of imine group (C=N) and a medium stretching band of C–N is observed at 1,005 cm^{-1} (Fig. 4). The adsorption of CV dye onto the adsorbent's surface shifted these stretching bands to 3,279; 2,896; 1,586; and 1,001 cm^{-1}, respectively.

The IR spectrum of MSA identifies the presence of the following functional groups: the broad band at 3,272 cm^{-1} indicates the presence of hydroxyl group (–OH), weak band at 2,906 cm^{-1} indicates that (C–H) bond of methyl group ($–CH_3$) is present, a medium stretching band at 1,586 cm^{-1} confirms the presence of imine group (C=N) and a medium stretching band of C–N is observed at 1,102 cm^{-1}. Slight changes in the wavenumbers were observed after treatment of CV dye: stretching bands of (–OH), (C–H), (C=N), and (C–N) at 3,267; 2,865; 1,577; and 1,004 cm^{-1}, respectively. The shifts observed in the IR bands indicate that these functional groups are probably involved in the adsorption of CV dye.

Fig. 5 shows the point of zero charge (pH_{pzc}) of SA is at pH 6.40 whereas the pH_{pzc} of MSA is at pH 5.00. At any pH below the pH_{pzc}, the surface of an adsorbent becomes more positively charged as a result of protonation and favors the adsorption of anionic substances, whereas, at pH higher than pH_{pzc}, deprotonation results in the surface of adsorbent causing it to become more negatively charged and attracts cationic substances in solution. Unlike reported adsorbents where base modified adsorbents showed a higher pH_{pzc}, it was observed in this study that base modification of SA sample has lowered the pH_{pzc} of SA from 6.4 to 5.0.

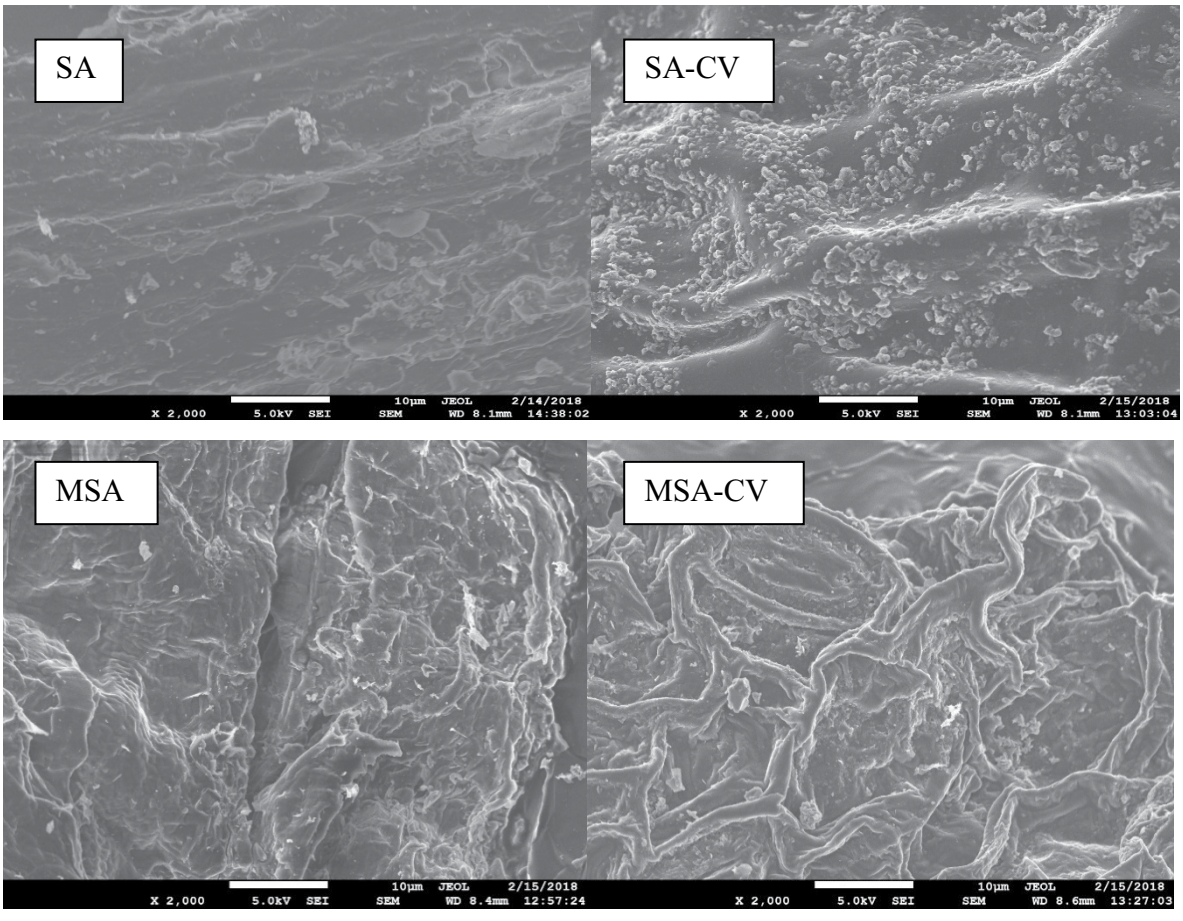

Fig. 3. SEM images of SA and MSA before and after adsorption of CV dye at ×2,000 magnification.

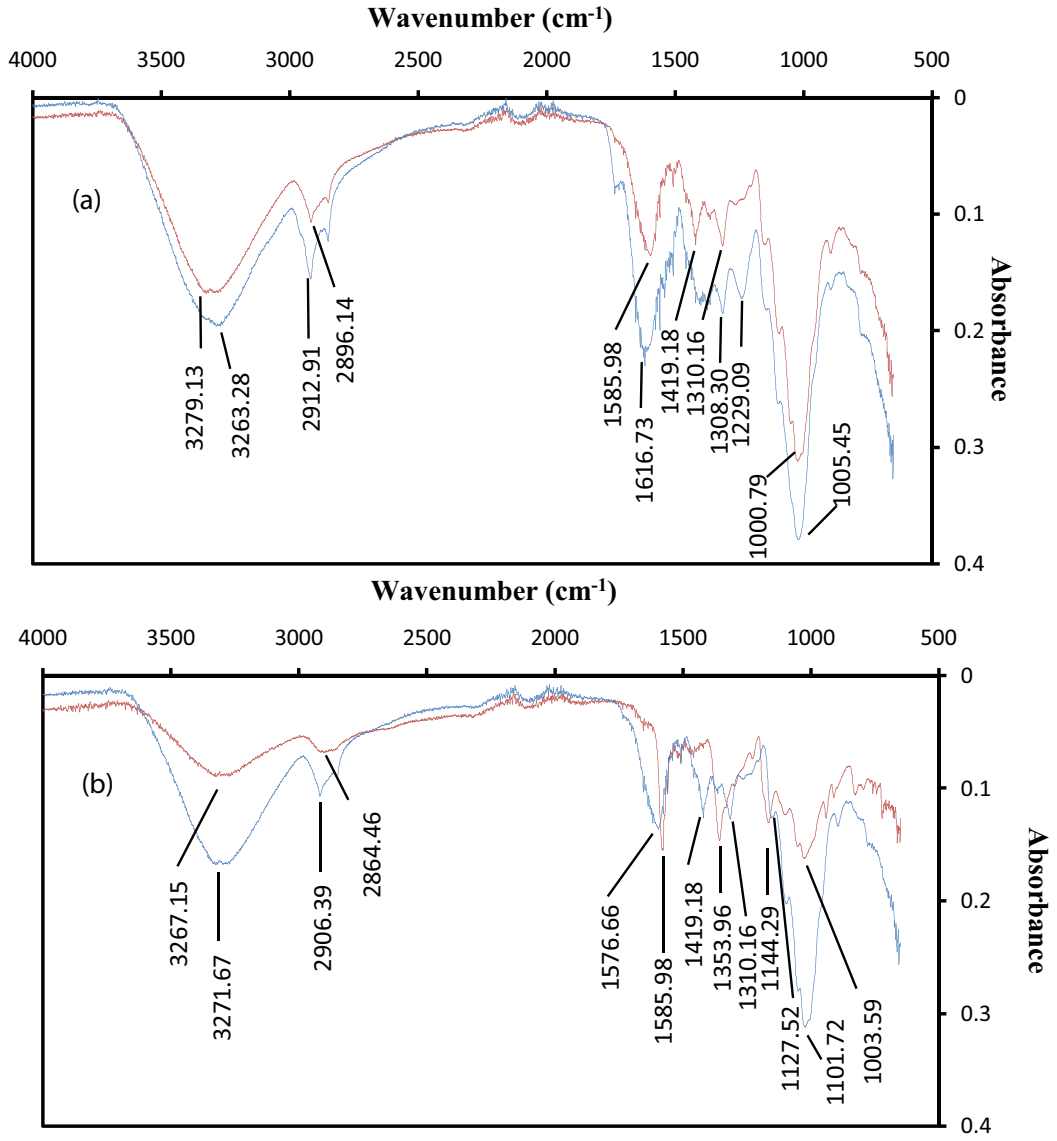

Fig. 4. FTIR spectra of (a) SA and (b) MSA before (—) and after (—) adsorption of CV dye.

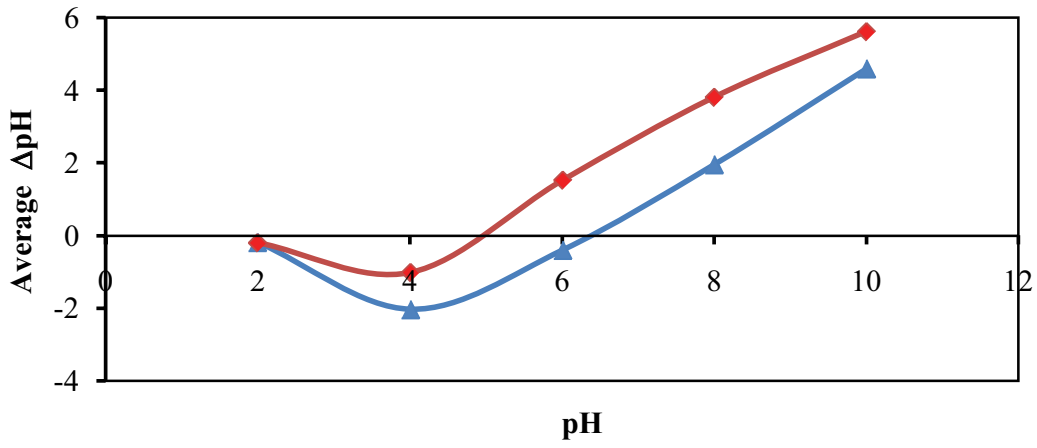

Fig. 5. Determination of pH_{pzc} for SA (—) and MSA (—).

This indicates that adsorbent's surface of SA was positively charged in the adsorption process, as the untreated (ambient) pH of CV dye was found to be at pH 5.05. Hence, there would be some electrostatic repulsion between the positively charged surface of SA and the cationic CV dye. This explains the more efficient adsorption of cationic CV dye by MSA as compared to SA, as shown by the higher maximum adsorption capacity (q_{max}) in the adsorption isotherm section.

3.2. Effects of experimental parameters on the extent of adsorption

3.2.1. Effect of contact time

The duration of contact time is an important parameter to investigate in adsorption studies as it provides information on the time needed for the adsorbent–adsorbate system to reach a state of equilibrium. In this study, during the first 30 min of contact time (Fig. 6), the adsorption of CV on the adsorbent increased rapidly due to the presence of high availability of active sites on the adsorbent's surface for adsorbates to bind to. Beyond 30 min, the adsorption rate abruptly decreased and showed insignificant increase in the amount of CV dye adsorbed until it reached equilibrium. This decrease in rate is due to the reduction in availability of vacant active sites for binding of adsorbates [47]. The contact time for SA and MSA to reach equilibrium was found to be 180 and 120 min, respectively.

3.2.2. Effect of medium pH

The pH of the system is a significant parameter in adsorption studies as it affects the surface charge of the adsorbent and the ionization of adsorbates. In this study, the extent of removal using 100 mg L^{-1} CV dye solution was investigated at pH 2.0, 4.0, 6.0, 8.0, 10.0, and 12.0. Results presented in Fig. 7 show that both SA and MSA gave similar trends, with the lowest removal of CV at pH 2.0. Compared to the ambient pH at pH 5.05, a reduction of approximately 64% and 46% were observed at pH 2.0 for SA and MSA, respectively. This could be attributed to the increased hydroxonium (H_3O^+) ions present in strong acidic condition which will cause the functional groups on the surface of adsorbent to be protonated, and thus, the adsorbent's surface will become positively charged. This in turn will lead to the electrostatic repulsion between positively charged surface and cationic CV dye, thereby lowering the extent of removal of the dye. Further, H_3O^+ ions will also compete with cationic CV dye for active sites in the adsorbent.

The percentage removal of SA and MSA rapidly increased when the pH of the system was changed from pH 2.0 to 4.0. Between pH 4.0 to pH 10.0, the increase in percentage removal of CV dye was insignificant; <3% for both adsorbents. The highest removal of CV for both adsorbents was at pH 12.0 which could be explained by the presence of OH^-, at which the functional groups on the adsorbent would be deprotonated. The negatively charged surface of adsorbent will favor adsorption as it is electrostatically attracted to cationic CV dye as they are oppositely charged.

3.2.3. Effect of salts (ionic strength)

Effect of ionic strength provides information on the extent of electrostatic interactions between the adsorbent and adsorbate in ionic environments. Such information is important when extended toward real applications because wastewater effluents containing dyes usually have salts present and these salts could occupy or compete for vacant sites on the surface of adsorbent during the adsorption process. Herein, according to the results shown in Fig. 8 for SA, the adsorption of CV on SA decreases, in general, upon addition of salts up to 1.0 M concentration, which is a fairly high concentration levels of ions as far as industrial effluents are concerned. This clearly shows the ionic environments block the diffusion of big molecules, such as CV dye, from the bulk to the adsorbent's surface. Further, when the concentration of salt is high, cations present in salt will compete and occupy the active sites where cationic CV dye was supposed to bind to. This would inhibit the adsorption of CV dye onto the adsorbent's surface and decrease the electrostatic interaction between adsorbent and adsorbate. However, the increase in the extent of dye removal in NaCl environments at concentrations beyond 0.1 M may be due to higher chloride levels which could attract positively

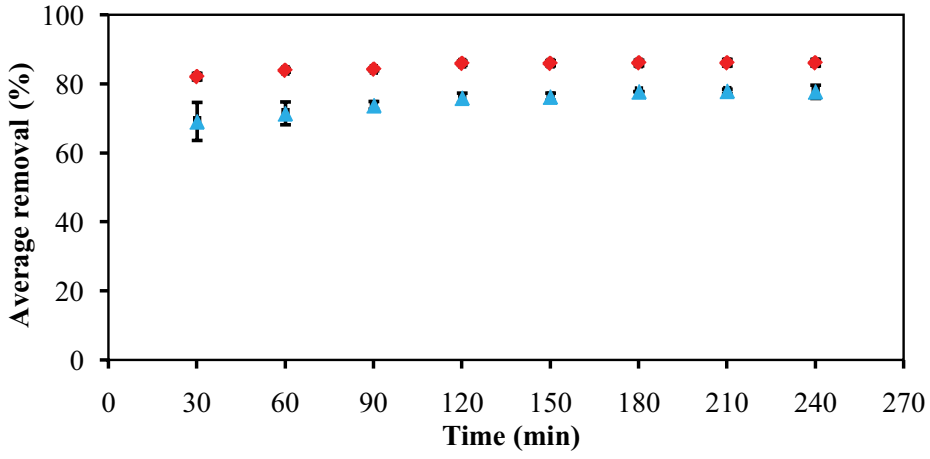

Fig. 6. Effect of contact time on the amount of CV dye adsorbed onto SA (▲) and MSA (◆) at room temperature.

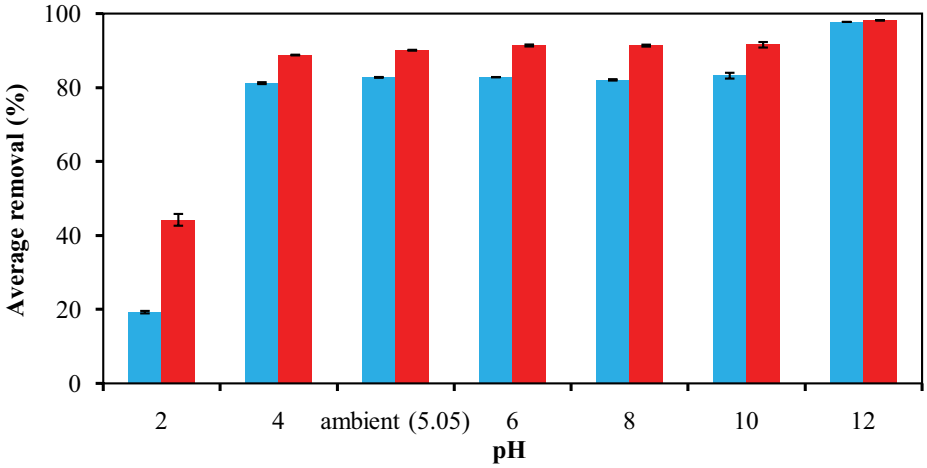

Fig. 7. Effect of pH on the removal of 100 mg L^{-1} CV dye by SA (■) and MSA (■) at ambient temperature.

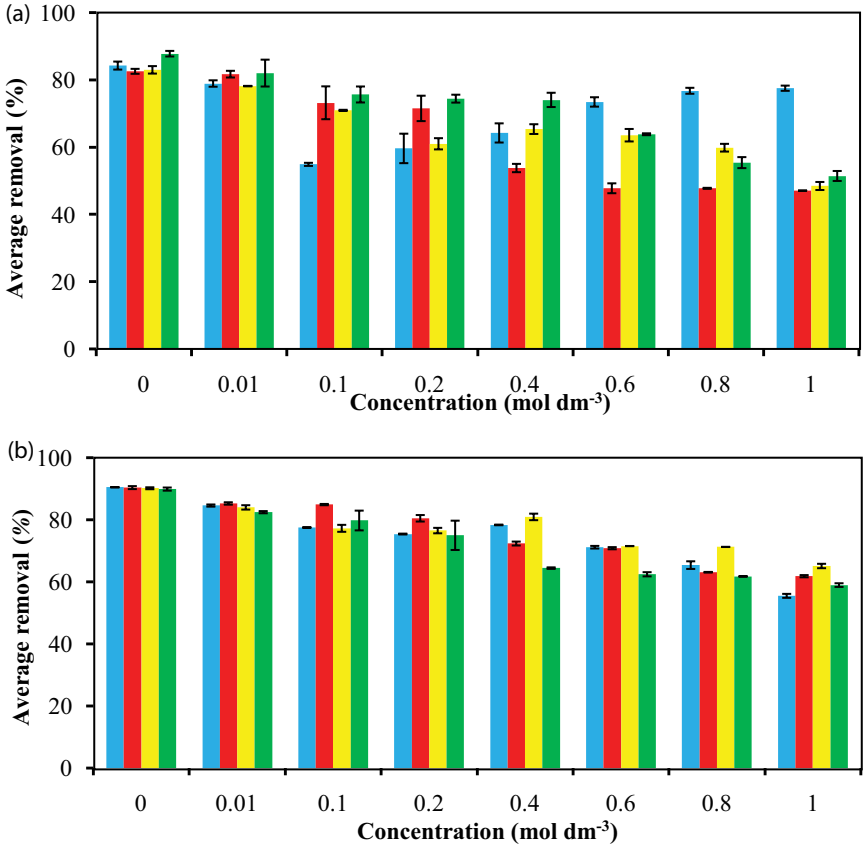

Fig. 8. Effect of ionic strength using NaCl (■), $NaNO_3$ (■), KCl (■) and KNO_3 (■) on the adsorption of CV dye by SA (a) and MSA (b).

charged CV dye molecules through Coulombic interactions. This argument is valid to some extent in the KCl medium where the extent of dye removal has increased from 0.2 M up to 0.8 M. Another fact to be considered is that the mechanism of adsorption may not purely depend on electrostatic interaction, and non-electrostatic interactions such as hydrophobic–hydrophobic interactions are also possible.

Such complications were not encountered when the adsorbent is MSA and the extent of dye removal decreases with increase in the ionic concentration in a more systematic manner. This is probably due to high concentration of surface negative charges created as a result of base treatment, thereby promoting stronger ionic interactions with the positively charged dye molecules, masking the effect

of bulk chloride ions to some extent. More importantly, the extent of dye removal by MSA did not go below 59% even at 1.0 M ionic environment, whereas in the presence of $NaNO_3$ and KNO_3 environments, the extent of dye removal by SA was below 50%. This clearly demonstrates the potential of MSA for removal of CV dye when present in ionic environments. Nevertheless, in the absence of ionic environments, both SA and MSA can be recommended.

3.3. Adsorption isotherm

The results obtained from the isotherm experiments are shown below in Fig. 9, and the data obtained were analyzed by the Langmuir [48], Freundlich [49], Temkin [50], Dubinin–Radushkevich (D–R) [51], Redlich–Peterson (R–P) [52], and Sips [53] isotherm models to predict the adsorption of CV dye onto SA and MSA. Six different error functions: average relative errors (ARE), sum of the square of the errors (ERRSQ), the hybrid fractional error function (HYBRID), Marquardt's percent standard deviation (MPSD), sum of absolute errors (EABS), and Chi-square test (χ^2) were also carried out on the various isotherm models. These isotherm models have been widely discussed [54].

Briefly, the Langmuir isotherm model describes the adsorption process based on the monolayer adsorption of adsorbate onto the adsorbent surface, in which there is no involvement in the interaction between adsorbate. Non-linear and linear forms of this model are given by Eqs. (3) and (4), respectively.

$$\text{Non-linear: } q_e = \frac{q_m K_L C_e}{1 + K_L C_e} \tag{3}$$

$$\text{Linearized: } \frac{C_e}{q_e} = \frac{1}{K_L q_m} + \frac{C_e}{q_m} \tag{4}$$

where q_m is the theoretical monolayer adsorption capacity of adsorbent in mg g^{-1}, q_e is experimental adsorbed dye in mg g^{-1}, K_L is the Langmuir adsorption constant in L mg^{-1}, and C_e is the final concentration of adsorbate in mg L^{-1}.

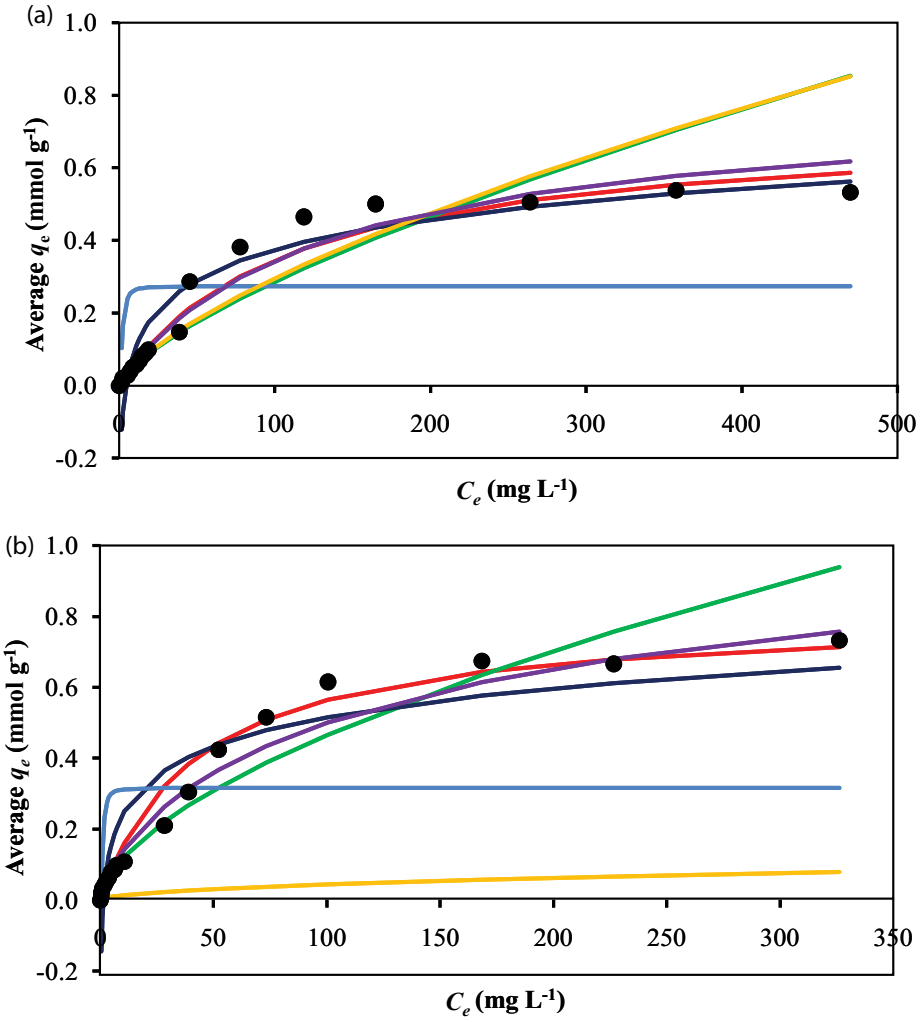

Fig. 9. Comparison of experimental q_e (●) with six isotherm models, namely Langmuir (▬), Freundlich (▬), Temkin (▬), D-R (▬), R-P (▬) and Sips (▬), for adsorption of CV onto SA (a) and MSA (b).

Another important parameter relevant to the Langmuir isotherm is the separation factor (R_L), a dimensionless constant used to find out if the Langmuir isotherm model is favorable. It can be calculated according to Eq. (5).

$$R_L = \frac{1}{\left(1 + K_L C_0\right)} \tag{5}$$

where C_0 is the initial concentration of adsorbate in mg L^{-1}. When $0 < R_L < 1$ provides favorable conditions, $R_L > 1$ indicates unfavorable, conditions, $R_L = 1$ is Langmuir linear, and $R_L = 1$, Langmuir irreversible.

The Freundlich adsorption isotherm assumes the adsorption takes place on a heterogeneous surface where it can adsorb more than a layer of adsorbate onto the adsorbent surface. This model suggests that increase in the concentration of adsorbate in the system will lead to the increase in adsorption of adsorbate onto the adsorbent surface. It assumes that availability of active sites on the adsorbent is unlimited. The Freundlich isotherm model can be described by Eqs. (6) and (7) listed below:

$$\text{Non-linear: } q_e = K_F C_e^{\frac{1}{n_F}} \tag{6}$$

$$\text{Linearized: } \ln q_e = \frac{1}{n_F}\ln C_e + \ln K_F \tag{7}$$

where q_e is experimental adsorbed dye in mg g^{-1}, K_F is the adsorption capacity of adsorbent in mg g^{-1} (L $mg^{-1})^{1/n}$, n_F is the Freundlich constant, and C_e is the final concentration of adsorbate in mg L^{-1}.

Unlike the Langmuir and Freundlich isotherms, the Temkin isotherm takes account of the interaction between the adsorbent and adsorbate. The model assumes the heat energy of adsorption of the adsorbate decreases linearly with the coverage. The equations of Temkin isotherm model are stated as Eqs. (8) and (9):

$$\text{Non-linear: } q_e = \frac{RT}{b_T}\ln K_T C_e \tag{8}$$

$$\text{Linearized: } q_e = \frac{RT}{b_T}\ln K_T + \frac{RT}{b_T}\ln C_e \tag{9}$$

where q_e is experimental adsorbed dye in mg g^{-1}, b_T is the Temkin constant in kJ mol^{-1}, K_T is the equilibrium binding constant, and C_e is the final concentration of adsorbate in mg L^{-1}.

Dubinin–Radushkevich isotherm is used to predict the adsorption mechanism with the observed energy of adsorption onto the heterogeneous surface. Eqs. (10)–(12) represent the isotherm model:

$$\ln q_e = \ln q_m - K_{\mathrm{DR}}\varepsilon^2 \tag{10}$$

where q_e is experimental adsorbed dye in mg g^{-1}, q_m is the theoretical isotherm adsorption capacity of adsorbent in mg g^{-1}, K_{DR} is the constant to adsorption energy in (mol $kJ^{-1})^2$, and ε is the D–R isotherm constant.

$$\varepsilon = RT\ln\left(1 + \frac{1}{C_e}\right) \tag{11}$$

where R is the gas constant (8.314 J mol^{-1} K^{-1}), T is the temperature in K, and C_e is the final concentration of adsorbate in mg L^{-1}.

$$E = \frac{1}{\sqrt{2K_{\mathrm{DR}}}} \tag{12}$$

From Eqs. (10) and (11), the mean free energy needed for adsorption of one molecule of adsorbate (E) in the solution to be transferred onto the adsorbent surface can be calculated.

The R–P is a three-parameter model, which is a combination of both Langmuir and Freundlich isotherm models. It does not completely obey any one of the monolayer and multi-layer adsorptions of Langmuir and Freundlich, as it approaches the Langmuir model at lower concentration of adsorbate and approaches the Freundlich model at high concentration of adsorbate. The equation for the R–P model is defined in Eqs. (13) and (14):

$$\text{Non-linear: } q_e = \frac{K_{\mathrm{RP}} C_e}{1 + \propto C_e^n} \tag{13}$$

$$\text{Linearized: } \ln\left(K_{\mathrm{RP}}\frac{C_e}{q_e} - 1\right) = n\cdot\ln C_e + \ln \propto \tag{14}$$

where q_e is experimental adsorbed dye in mg g^{-1}, K_{RP} and α is the R–P constant, n is the exponent that lies between 0 and 1, and C_e is the final concentration of adsorbate in mg L^{-1}.

The Sips isotherm is another three-parameter isotherm model which combines the features of Langmuir and Freundlich isotherm model, which predicts the Freundlich adsorption at low adsorbate concentrations and Langmuir adsorption at higher concentrations. This model is described by Eqs. (15) and (16):

$$\text{Non-linear: } q_e = \frac{K_S C_e^{\beta_s}}{1 - a_S C_e^{\beta_s}} \tag{15}$$

$$\text{Linearized: } \beta_S \ln C_e = -\ln\left(\frac{K_S}{q_e}\right) + \ln a_S \tag{16}$$

where q_e is experimental adsorbed dye in mg g^{-1}, K_S is the Sips isotherm constant in L g^{-1}, β_S is the exponent of Sips isotherm, a_S is the Sips isotherm model constant in L g^{-1}, and C_e is the final concentration of adsorbate in mg L^{-1}.

Different error functions which can be calculated using Eqs. (17)–(19) listed below [54] can be used to identify which isotherm model best describes the experimental data obtained from isotherm experiments. The smaller the error

functions, the closer the isotherm model to the experimental curve.

- Average relative errors (ARE):

$$\text{ARE} = \frac{100}{n}\sum_{i=1}^{n}\left[\frac{\left(q_{e,\text{calc}} - q_{e,\text{meas}}\right)^2}{q_{e,\text{meas}}}\right] \quad (17)$$

- Sum of absolute errors (EABS):

$$\text{EABS} = \sum_{i=1}^{p}\left[q_{e,\text{meas}} - q_{e,\text{calc}}\right] \quad (18)$$

- Chi-square test (χ^2):

$$\chi^2 : \sum_{i=1}^{n}\frac{\left(q_{e,\text{meas}} - q_{e,\text{calc}}\right)^2}{q_{e,\text{meas}}} \quad (19)$$

where $q_{e,\text{meas}}$ is the experimental adsorption capacity in mg g^{-1}, $q_{e,\text{calc}}$ is the calculated adsorption capacity isotherm model in mg g^{-1}, n is the number of data points, and p is the number of parameters.

From Fig. 9, it was found that the amount of CV dye adsorbed onto the MSA was higher as compared to SA. In order to find the best-fitted isotherm model for the experimental data, the isotherm model should be closest to the experimental graph of q_e vs. C_e, having the highest R^2 value and the lowest error values. From the simulation plots of various isotherm models in Fig. 9, the Freundlich, D–R, and R–P isotherm models show clear deviation from the experimental data leaving only the Langmuir, Temkin, and Sips isotherm models being possible. Table 1 shows the R^2 value of the Temkin model (0.9145) is relatively lower than that of the Langmuir (0.9678) and Sips (0.9761) models. The R^2 value of Sips isotherm was the highest whereas the errors of Langmuir isotherm are the lowest as shown in Table 1. However, the difference in error functions of the Langmuir and Sips isotherms was small and comparable. Therefore, the above comparisons point toward the conclusion that the adsorption mechanism of CV by SA adsorbent is best described by both the Langmuir and Sips isotherm models.

Fig. 9 shows that MSA adsorbent shifted the Temkin isotherm model and caused slight deviation from the experimental plot. In this case, plot of q_e against C_e eliminated four of the isotherm models: the Freundlich, D–R, R–P, and Temkin. Comparison of the R^2 and errors were done. Although the Langmuir and Sips isotherm models have

Table 1
Isotherm values of each model for adsorption of CV on SA and MSA adsorbents

Model	SA	MSA
Langmuir		
$q_{\max}$ (mmol g^{-1})	0.72	0.81
$q_{\max}$ (mg g^{-1})	294.35	329.17
K_L (L mmol^{-1})	0.01	0.02
R^2	0.9678	0.9821
R_L	0.10–0.92	0.04–0.82
ARE	12.43	19.32
EABS	0.48	0.46
χ^2	0.23	0.13
Freundlich		
K_F (mmol g^{-1} (L mmol^{-1})$^{1/n}$)	0.01	12.34
n	1.41	1.68
R^2	0.9522	0.9759
ARE	19.10	13.20
EABS	1.10	0.81
χ^2	0.56	0.44
Temkin		
K_T (L mmol^{-1})	0.22	0.78
b_T (kJ mol^{-1})	20.49	20.97
R^2	0.9145	0.8822
ARE	127.80	159.33
EABS	0.93	1.52
χ^2	1.61	2.39
Dubinin–Radushkevich		
$q_{\max}$ (mmol g^{-1})	0.27	0.32
$q_{\max}$ (mg g^{-1})	111.60	128.73
B (J mol^{-1})	7.04×10^{-7}	2.42×10^{-7}
E (kJ mol^{-1})	842.59	1,437.96
R^2	0.7231	0.7303
ARE	258.07	159.77
EABS	3.23	3.48
χ^2	6.01	4.48
Redlich–Peterson		
K_R (L g^{-1})	0.02	0.01
α	0.36	0.51
a_R (L mmol^{-1})	1.12	2.39
R^2	0.7882	0.9464
ARE	17.82	85.24
EABS	1.07	4.32
χ^2	0.53	4.64
Sips		
$q_{\max}$ (mmol g^{-1})	0.80	1.20
$q_{\max}$ (mg g^{-1})	326.38	489.58
K_S (L mmol^{-1})	0.01	0.02
$1/n$	0.97	0.74
n	1.03	1.35
R^2	0.9761	0.9824
ARE	12.46	13.04
EABS	0.54	0.51
χ^2	0.24	0.23

comparable R^2 values for adsorption of CV by MSA, few error functions of the Langmuir isotherm are much greater as compared to those of the Sips isotherm. For instance, ARE in Langmuir and Sips are 19.32 and 13.04, respectively; MPSD in Langmuir and Sips were 29.15 and 17.48, respectively. Due to the large difference in error values, the Sips isotherm model with its lower error values can be taken as the better fitted model to describe the adsorption system under investigation.

By comparing the isotherm modeling for both SA and MSA systems, it can be argued that adsorption of CV dye on both SA and MSA can be explained by both monolayer and multilayer adsorption, and that the values obtained by the Sips isotherm modeling can be used. Accordingly, the q_{max} value of SA (326.38 mg g^{-1}) is greater than that of many reported adsorbents, such as activated carbon, peat, and fruit wastes, as reported in Table 2. Upon treatment with NaOH, the modified MSA shows further enhancement of its q_{max} value by 50%, which is a significant achievement of this research. These results conclusively demonstrate that both SA and MSA are strong adsorbents for CV, and that these adsorbents have potential as new low-cost adsorbents for large-scale removal of CV dye even when present in ionic environments.

3.4. Effects of temperature

Adsorption of CV on SA and MSA investigated within the temperature range between 298 and 343 K using 100 and 500 mg L^{-1} CV dye solutions shows that the extent of adsorption decreased with increase in temperature, indicating that the adsorption process is exothermic (Fig. 10). This is favorable when applied to wastewater treatment because no heating is required to enhance the adsorption of dye, making the removal process more economical.

3.5. Regeneration study

Improper disposal of adsorbents after the adsorption process can also be considered as hazardous materials or secondary pollutants that cause environmental issues [77]. Therefore, regeneration or reuse of adsorbent is important to minimize expenses on proper disposal of adsorbent. Over the years, although there have been many reports on

Table 2
Comparison of q_{max} values in (mg g^{-1}) on different adsorbents on CV dye

Adsorbent	q_{max} (mg g^{-1})	References
Sauropus androgynous	326.4	This study
NaOH modified *Sauropus androgynous*	489.6	This study
Activated carbon (Ag nanoparticle immobilized)	87.2	[55]
Activated carbon (Chitosan composite)	0.3	[56]
Artocarpus odoratissimus (Tarap) core	217.0	[57]
Artocarpus odoratissimus leaf	50.5	[58]
Bentonite	105.3	[59]
Gum arabic-cl-poly(acrylamide) nanohydrogel	90.9	[60]
Artocarpus odoratissimus skin	118.0	[61]
NaOH modified *Artocarpus odoratissimus* skin	195.0	[61]
Artocarpus altilis (Breadfruit) skin	145.8	[62]
Montmorillonite	370.4	[63]
Acid modified montmorillonite	400.0	[63]
Artocarpus odoratissimus leaf-based cellulose	239.0	[64]
Cucumis sativus peel	149.3	[65]
Momordica charantia (bitter gourd) waste	244.8	[66]
NaOH modified rice husk	44.9	[67]
Artcoarpus camansi peel	275.0	[68]
NaOH modified *Artcoarpus camansi* peel	479.0	[68]
Heat treated halloysite	190.0	[69]
EDTA/graphene oxide corncob	95.9	[70]
Peat	108.0	[71]
Yeast treated peat	18.0	[72]
Bio-compatible self-assembled peptide fibrils	625.0	[73]
Dendritic post-cross-linked resin	497.5	[74]
Diplazium esculentum	350.9	[75]
Untreated almond shell	114.0	[76]
NaOH treated almond shell	123.0	[76]

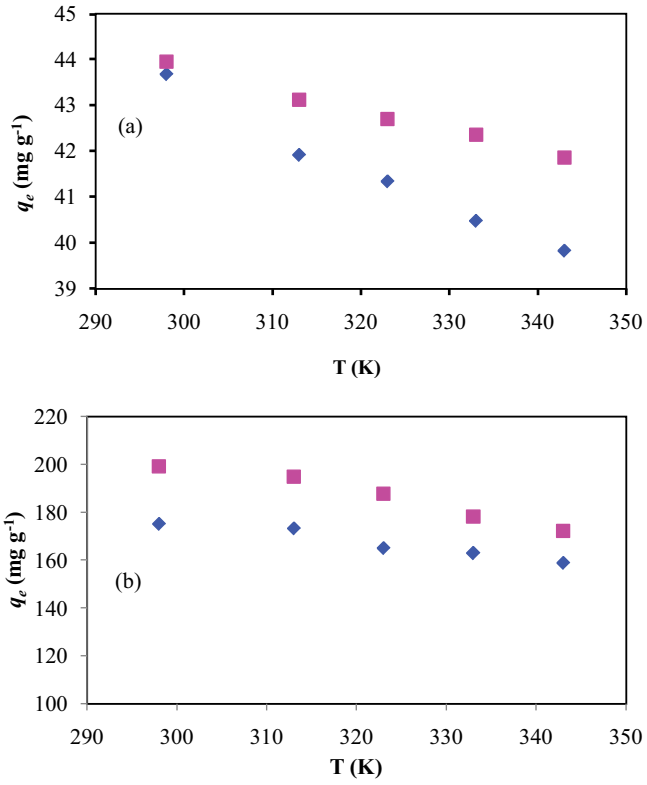

Fig. 10. Effects of temperature on the adsorption of CV onto SA (■) and MSA (◆) using (a) 100 mg L^{-1} and (b) 500 mg L^{-1} CV.

the use of adsorbents to remove pollutants, however many of these reports have excluded the study on the reusability of these spent adsorbents [78–81]. Regeneration of SA and MSA was done in this study by treatment of acid, base and water. As shown in Fig. 11, both SA and MSA could be regenerated, where acid and base being the more suitable washing solutions for desorption of adsorbates from the adsorbents. In regeneration of both SA and MSA adsorbents, the results showed an overall decrease throughout the five cycles. However, the percentage removal of SA adsorbent during acid and base washings were still 26.5% and 28.7%; percentage removal of MSA adsorbent during acid and base washings were higher compared to the SA adsorbent, which were 30.3% and 35.3%. Washing of adsorbents by using distilled water did not really regenerate the adsorbents, in this case, as it yielded a very low percentage removal, which was only around 10% removal for both SA and MSA. However, it must be stressed that high CV concentration (800 mg L^{-1}) was used in this study and therefore, for SA and MSA to still adsorb even after five cycles further confirms their ability to be regenerated and reused. In contrast, many adsorbents showed much reduced adsorption after a few cycles even when low dye concentrations were used [82].

4. Conclusion

Waste parts of the plant SA have been proven to be a potential, new and efficient low-cost adsorbent for the removal of CV dye from aqueous solution, with an adsorption capacity of 326.38 mg g^{-1} according to the Sips isotherm

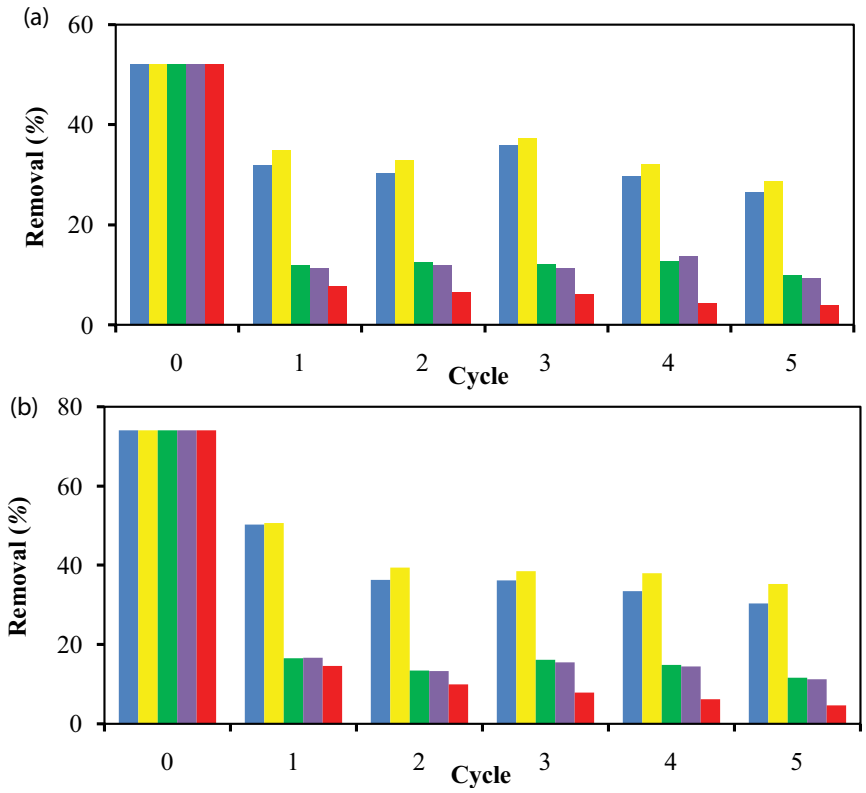

Fig. 11. Regeneration studies of SA (a) and MSA (b) showing treatment with acid (■), base (■), distilled water (■), quick wash with distilled water (■) and control (■).

model which is valid based on non-linear curve fitting and error function determinations. This value is superior to many other adsorbents reported. Further, modified SA (MSA), successfully and easily prepared by treatment with 1.0 M NaOH, shows a much better adsorption capacity of 489.58 mg g^{-1}, indicating 50% enhancement due to simple base treatment. The time taken for SA and MSA adsorbents to reach equilibrium was found to be 180 and 120 min, respectively. Highest percentage removal of adsorbate from the systems for both SA and MSA were at pH 12, where there is no competition of cationic CV dyes and H_3O^+ ions for active sites on the adsorbent's surface. When the concentration of salts present in an aqueous solution is high, it shows an overall decrease in the percentage removal of CV dye. However, the removal was not totally inhibited, and SA and MSA were still able to remove at least 47% of dye present in the system. More importantly, MSA is more tolerant to ionic environments compared to SA. The temperature dependant experiment also shows that the adsorption process is exothermic. The SA and MSA can be easily regenerated by using acid and base as washing solutions. The above findings therefore indicate that both SA and MSA are potential candidates to be applied as adsorbents in real life wastewater treatment. Various chemical treatments can be studied for the modification of SA, which could include acid, chelating agents and surfactants to see if such methods could result in the enhancement of adsorption. Therefore, SA can be further examined and investigated for its potential as an alternative to commercial adsorbent as compared to base modified.

Acknowledgments

The authors thank the Government of Brunei Darussalam and the Universiti Brunei Darussalam for their continuous support.

References

[1] S. Srivastava, R. Sinha, D. Roy, Toxicological effects of malachite green, Aquat. Toxicol., 66 (2004) 319–329.
[2] R. Kant, Textile dyeing industry an environmental hazard, Nat. Sci., 4 (2012) 22–26.
[3] B. de Campos Ventura-Camargo, M.A. Marin-Morales, Azo dyes: characterization and toxicity – a review, Text. Light Ind. Sci. Technol., 2 (2013) 85–103.
[4] R. Docampo, S.N.J. Moreno, The metabolism and mode of action of gentian violet, Drug Metab. Rev., 22 (1990) 161–178.
[5] J.A.Z. Egurrola, C.P. Pena, A.A. Echevarria, R.L. Ibarguren, P.A. Erbina, G.E. Olartecoechea, Glans penis necrosis secondary to gentian violet treatment, Arch. Esp. Urol., 42 (1989) 800–802.
[6] L.W.C. Tom, Ototoxicity of common topical antimycotic preparations, Laryngoscope, 110 (2000) 509–516.
[7] A. Aidoo, N. Gao, R.E. Neft, H.M. Schol, B.S. Hass, T.Y. Minor, R.H. Heflich, Evaluation of the genotoxicity of gentian violet in bacterial and mammalian cell systems, Teratog., Carcinog., Mutagen., 10 (1990) 449–462.
[8] W. Au, S. Pathak, C.J. Collie, T.C. Hsu, Cytogenetic toxicity of gentian violet and crystal violet on mammalian cells *in vitro*, Mutat. Res. Toxicol., 58 (1978) 269–276.
[9] S. Mani, R.N. Bharagava, Exposure to Crystal Violet, Its Toxic, Genotoxic and Carcinogenic Effects on Environment and Its Degradation and Detoxification for Environmental Safety, P. de Voogt, Ed., Reviews of Environmental Contamination and Toxicology, Vol. 237, Springer, Cham, 2016, pp. 71–104.
[10] V. Katheresan, J. Kansedo, S.Y. Lau, Efficiency of various recent wastewater dye removal methods: a review, J. Environ. Chem. Eng., 6 (2018) 4676–4697.
[11] M.A. Rauf, S. Salman Ashraf, Survey of recent trends in biochemically assisted degradation of dyes, Chem. Eng. J., 209 (2012) 520–530.
[12] T.H. Bokhari, N. Ahmad, M.I. Jilani, M. Saeed, UV/H_2O_2, UV/H_2O_2/SnO_2 and Fe/H_2O_2 based advanced oxidation processes for the degradation of disperse violet 63 in aqueous medium, Mater. Res. Express, 7 (2020), doi: 10.1088/2053-1591/ab6c15.
[13] M. Rahmat, A. Rehman, S. Rahmat, H.N. Bhatti, M. Iqbal, W.S. Khan, S.Z. Bajwa, R. Rahmat, A. Nazir, Highly efficient removal of crystal violet dye from water by MnO_2 based nanofibrous mesh/photocatalytic process, J. Mater. Res. Technol., 8 (2019) 5149–5159.
[14] A. Jamil, T.H. Bokhari, T. Javed, R. Mustafa, M. Sajid, S. Noreen, M. Zuber, A. Nazir, M. Iqbal, M.I. Jilani, Photocatalytic degradation of disperse dye violet-26 using TiO_2 and ZnO nanomaterials and process variable optimization, J. Mater. Res. Technol., 9 (2020) 1119–1128.
[15] R. Arshad, T.H. Bokhari, K.K. Khosa, I.A. Bhatti, M. Munir, M. Iqbal, D.N. Iqbal, M.I. Khan, M. Iqbal, A. Nazir, Gamma radiation induced degradation of anthraquinone reactive blue-19 dye using hydrogen peroxide as oxidizing agent, Radiat. Phys. Chem., 168 (2020), doi: 10.1016/j.radphyschem.2019.108637.
[16] N.U.H. Khan, H.N. Bhatti, M. Iqbal, A. Nazir, Decolorization of basic turquise blue X-GB and basic blue X-GRRL by the Fenton's process and its kinetics, Z. Phys. Chem., 233 (2019) 361–373.
[17] N.B. Singh, G. Nagpal, S. Agrawal, Rachna, Water purification by using adsorbents: a review, Environ. Technol. Innovation, 11 (2018) 187–240.
[18] L.B.L. Lim, N. Priyantha, Y.C. Lu, N.A.H.M. Zaidi, Adsorption of heavy metal lead using *Citrus grandis* (Pomelo) leaves as low-cost adsorbent, Desal. Water Treat., 166 (2019) 44–52.
[19] Z. Shamsollahi, A. Partovinia, Recent advances on pollutants removal by rice husk as a bio-based adsorbent: a critical review, J. Environ. Manage., 246 (2019) 314–323.
[20] N. Priyantha, L.B.L. Lim, N.H.M. Mansor, A.B. Liyandeniya, Irreversible sorption of Pb(II) from aqueous solution on breadfruit peel to mitigate environmental pollution problems, Water Sci. Technol., 80 (2019) 2241–2249.
[21] M. Zendehdel, M. Ramezani, B. Shoshtari-Yeganeh, G. Cruciani, A. Salmani, Simultaneous removal of Pb(II), Cd(II) and bacteria from aqueous solution using amino-functionalized Fe_3O_4/NaP zeolite nanocomposite, Environ. Technol., 40 (2019) 3689–3704.
[22] J. Mo, Q. Yang, N. Zhang, W. Zhang, Y. Zheng, Z. Zhang, A review on agro-industrial waste (AIW) derived adsorbents for water and wastewater treatment, J. Environ. Manage., 227 (2018) 395–405.
[23] A. Nazir, F. Zahra, M.U. Sabri, A. Ghaffar, A.Q. Ather, M.I. Khan, M. Iqbal, Charcoal prepared from bougainvillea spectabilis leaves as low cost adsorbent: kinetic and equilibrium studies for removal of iron from aqueous solution, Z. Phys. Chem., (2019) 1–15.
[24] A. Aichour, H. Zaghouane-Boudiaf, Highly brilliant green removal from wastewater by mesoporous adsorbents: kinetics, thermodynamics and equilibrium isotherm studies, Microchem. J., 146 (2019) 1255–1262.
[25] L.B.L. Lim, N. Priyantha, Y.C. Lu, N.A.H.M. Zaidi, Effective removal of methyl violet dye using pomelo leaves as a new low-cost adsorbent, Desal. Water Treat., 110 (2018) 264–274.
[26] A.G. Adeniyi, J.O. Ighalo, Biosorption of pollutants by plant leaves: an empirical review, J. Environ. Chem. Eng., 7 (2019), doi: 10.1016/j.jece.2019.103100.
[27] L.B.L. Lim, N. Priyantha, S.A.A. Latip, Y.C. Lu, A.H. Mahadi, Converting *Hylocereus undatus* (White dragon fruit) peel waste into a useful potential adsorbent for the removal of toxic congo red dye, Desal. Water Treat., 185 (2020) 307–317.
[28] A.M. Awad, R. Jalab, A. Benamor, M.S. Nasser, M.M. Ba-Abbad, M. El-Naas, A.W. Mohammad, Adsorption of organic pollutants by nanomaterial-based adsorbents: an overview, J. Mol. Liq., 301 (2020), doi: 10.1016/j.molliq.2019.112335.

[29] M.R.R. Kooh, M.K. Dahri, L.B.L. Lim, Removal of methyl violet 2B dye from aqueous solution using *Nepenthes rafflesiana* pitcher and leaves, Appl. Water Sci., 7 (2017) 3859–3868.
[30] M.K. Dahri, L.B.L. Lim, C.C. Mei, Cempedak durian as a potential biosorbent for the removal of brilliant green dye from aqueous solution: equilibrium, thermodynamics and kinetics studies, Environ. Monit. Assess., 187 (2015), doi: 10.1007/s10661-015-4768-z.
[31] M.R.R. Kooh, M.K. Dahri, L.B.L. Lim, L.H. Lim, Batch adsorption studies on the removal of acid blue 25 from aqueous solution using *Azolla pinnata* and soya bean waste, Arabian J. Sci. Eng., 41 (2016) 2453–2464.
[32] S. Dawood, T.K. Sen, Removal of anionic dye congo red from aqueous solution by raw pine and acid-treated pine cone powder as adsorbent: equilibrium, thermodynamic, kinetics, mechanism and process design, Water Res., 46 (2012) 1933–1946.
[33] M. Jafari, M.R. Rahimi, M. Ghaedi, K. Dashtian, ZnO nanoparticles loaded different mesh size of porous activated carbon prepared from *Pinus eldarica* and its effects on simultaneous removal of dyes: multivariate optimization, Chem. Eng. Res. Des., 125 (2017) 408–421.
[34] H.N. Bhatti, Y. Safa, S.M. Yakout, O.H. Shair, M. Iqbal, A. Nazir, Efficient removal of dyes using carboxymethyl cellulose/alginate/polyvinyl alcohol/rice husk composite: adsorption/desorption, kinetics and recycling studies, Int. J. Biol. Macromol., 150 (2020) 861–870.
[35] M. Ahmad, G. Abbas, R. Haider, F. Jalal, G.A. Shar, G.A. Soomro, N. Qureshi, M. Iqbal, A. Nazir, Kinetics and equilibrium studies of *Eriobotrya japonica*: a novel adsorbent preparation for dyes sequestration, Z. Phys. Chem., 233 (2019) 1469–1484.
[36] K. Saeed, M. Ishaq, S. Sultan, I. Ahmad, Removal of methyl violet 2B from aqueous solutions using untreated and magnetite-impregnated almond shell as adsorbents, Desal. Water Treat., 57 (2016) 13484–13493.
[37] A. Kausar, K. Naeem, M. Tariq, Z.I.H. Nazli, H.N. Bhatti, F. Jubeen, A. Nazir, M. Iqbal, Preparation and characterization of chitosan/clay composite for direct rose FRN dye removal from aqueous media: comparison of linear and non-linear regression methods, J. Mater. Res. Technol., 8 (2019) 1161–1174.
[38] H. Khoo, A. Azlan, A. Ismaila, *Sauropus androgynus* leaves for health benefits: hype and the science, Nat. Prod. J., 5 (2015) 115–123.
[39] H. Bunawan, S.N. Bunawan, S.N. Baharum, N.M. Noor, *Sauropus androgynus* (L.) Merr. induced bronchiolitis obliterans: from botanical studies to toxicology, Evid. Based Complement Alternat. Med., 2015 (2015) 1–7.
[40] N. Andarwulan, D. Kurniasih, R.A. Apriady, H. Rahmat, A.V. Roto, B.W. Bolling, Polyphenols, carotenoids, and ascorbic acid in underutilized medicinal vegetables, J. Funct. Foods, 4 (2012) 339–347.
[41] S.F. Yu, T.M. Chen, Y.H. Chen, Apoptosis and necrosis are involved in the toxicity of *Sauropus androgynus* in an *in vitro* study, J. Formos. Med. Assoc., 106 (2007) 537–547.
[42] L.B.L. Lim, N. Priyantha, X.H. Bong, N.A.H.M. Zaidi, Enhancement of adsorption characteristics of methyl violet 2B dye through NaOH treatment of *Cucumis melo var. cantalupensis* (rock melon) skin, Desal. Water Treat., 180 (2020) 336–348.
[43] N.A.H.M. Zaidi, L.B.L. Lim, A. Usman, Enhancing adsorption of malachite green dye using base-modified *Artocarpus odoratissimus* leaves as adsorbents, Environ. Technol. Innovation, 13 (2019) 211–223.
[44] L.B.L. Lim, N. Priyantha, N.A.H.M. Zaidi, A superb modified new adsorbent, *Artocarpus odoratissimus* leaves, for removal of cationic methyl violet 2B dye, Environ. Earth Sci., 75 (2016), doi: 10.1007/s12665-016-5969-7.
[45] T. Zehra, N. Priyantha, L.B.L. Lim, E. Iqbal, Sorption characteristics of peat of Brunei Darussalam V: removal of congo red dye from aqueous solution by peat, Desal. Water Treat., 54 (2015) 2592–2600.
[46] M.K. Dahri, H.I. Chieng, L.B.L. Lim, N. Priyantha, C.C. Mei, Cempedak durian (*Artocarpus* sp.) peel as a biosorbent for the removal of toxic methyl violet 2B from aqueous solution, Korean Chem. Eng. Res., 53 (2015) 576–583.
[47] P. Das Saha, S. Chowdhury, M. Mondal, K. Sinha, Biosorption of direct red 28 (Congo Red) from aqueous solutions by eggshells: batch and column studies, Sep. Sci. Technol., 47 (2012) 112–123.
[48] I. Langmuir, The adsorption of gases on plane surfaces of glass, mica and platinum, J. Am. Chem. Soc., 40 (1918) 1361–1403.
[49] H.M.F. Freundlich, Over the adsorption in solution, J. Phys. Chem., 57 (1906) 1100–1107.
[50] M.J. Temkin, V. Pyzhev, Kinetics of ammonia synthesis on promoted iron catalysts, Acta. Physiochim., 12 (1940).
[51] M.M. Dubinin, L.V. Radushkevich, The equation of the characteristic curve of activated charcoal, Dokl. Akad. Nauk. SSSR, 55 (1947) 327–329.
[52] D.L. Peterson, O. Redlich, A useful adsorption isotherm, J. Phys. Chem., 63 (1959), doi: 10.1021/j150576a611.
[53] R. Sips, Combined form of Langmuir and Freundlich equations, J. Chem. Phys., 16 (1948) 490–495.
[54] N. Ayawei, A.N. Ebelegi, D. Wankasi, Modelling and interpretation of adsorption isotherms, J. Chem., 2017 (2017) 1–11.
[55] A.H. AbdEl-Salam, H.A. Ewais, A.S. Basaleh, Silver nanoparticles immobilised on the activated carbon as efficient adsorbent for removal of crystal violet dye from aqueous solutions a kinetic study, J. Mol. Liq., 248 (2017) 833–841.
[56] H. Jayasantha Kumari, P. Krishnamoorthy, T.K. Arumugam, S. Radhakrishnan, D. Vasudevan, An efficient removal of crystal violet dye from waste water by adsorption onto TLAC/chitosan composite: a novel low cost adsorbent, Int. J. Biol. Macromol., 96 (2017) 324–333.
[57] M.K. Dahri, M.R.R. Kooh, L.B.L. Lim, *Artocarpus odoratissimus* (Tarap) core as an adsorbent for the removal of crystal violet dye from aqueous solution, J. Mater. Environ. Sci., 8 (2017) 3706–3717.
[58] L.B.L. Lim, N. Priyantha, H.H. Cheng, N.A.H.M. Zaidi, Adsorption characteristics of *Artocarpus odoratissimus* leaf toward removal of toxic crystal violet dye: isotherm, thermodynamics and regeneration studies, J. Environ. Biotechnol. Res., 4 (2016) 32–40.
[59] N.R.E. Radwan, M.E. Hagar, K. Chaieb, Adsorption of crystal violet dye on modified bentonites, Asian J. Chem., 28 (2016) 1643–1647.
[60] G. Sharma, A. Kumar, M. Naushad, A. García-Peñas, A.H. Al-Muhtaseb, A.A. Ghfar, V. Sharma, T. Ahamad, F.J. Stadler, Fabrication and characterization of gum arabic-cl-poly(acrylamide) nanohydrogel for effective adsorption of crystal violet dye, Carbohydr. Polym., 202 (2018) 444–453.
[61] L.B.L. Lim, N. Priyantha, T. Zehra, C.W. Then, C.M. Chan, Adsorption of crystal violet dye from aqueous solution onto chemically treated *Artocarpus odoratissimus* skin: equilibrium, thermodynamics, and kinetics studies, Desalin. Water Treat., 57 (2016) 10246–10260.
[62] L.B.L. Lim, N. Priyantha, N.H.M. Mansor, *Artocarpus altilis* (Breadfruit) skin as a potential low-cost biosorbent for the removal of crystal violet dye: equilibrium, thermodynamics and kinetics studies, Environ. Earth Sci., 73 (2015) 3239–3247.
[63] G.K. Sarma, S. Sen Gupta, K.G. Bhattacharyya, Adsorption of crystal violet on raw and acid-treated montmorillonite, K10, in aqueous suspension, J. Environ. Manage., 171 (2016) 1–10.
[64] N.A.H.M. Zaidi, L.B.L. Lim, A. Usman, *Artocarpus odoratissimus* leaf-based cellulose as adsorbent for removal of methyl violet and crystal violet dyes from aqueous solution, Cellulose, 25 (2018) 3037–3049.
[65] S. Shakoor, A. Nasar, Utilization of cucumis sativus peel as an eco-friendly biosorbent for the confiscation of crystal violet dye from artificially contaminated wastewater, Anal. Chem. Lett., 9 (2019) 1–19.
[66] L.B.L. Lim, N. Priyantha, K.J. Mek, N.A.H.M. Zaidi, Potential use of *Momordica charantia* (bitter gourd) waste as a low-cost adsorbent to remove toxic crystal violet dye, Desal. Water Treat., 82 (2017) 121–130.
[67] S. Chakraborty, S. Chowdhury, P. Das Saha, Adsorption of crystal violet from aqueous solution onto NaOH-modified rice husk, Carbohydr. Polym., 86 (2011) 1533–1541.
[68] H.I. Chieng, L.B.L. Lim, N. Priyantha, Enhancement of crystal violet dye adsorption on *Artocarpus camansi* peel through

sodium hydroxide treatment, Desal. Water Treat., 58 (2017) 320–331.
[69] A.A. Krasilin, D.P. Danilovich, E.B. Yudina, S. Bruyere, J. Ghanbaja, V.K. Ivanov, Crystal violet adsorption by oppositely twisted heat-treated halloysite and pecoraite nanoscrolls, Appl. Clay Sci., 173 (2019) 1–11.
[70] H. Wang, X. Lai, W. Zhao, Y. Chen, X. Yang, X. Meng, Y. Li, Efficient removal of crystal violet dye using EDTA/Graphene oxide functionalized corncob: a novel low cost adsorbent, RSC Adv., 9 (2019) 21996–22003.
[71] H.I. Chieng, L.B.L. Lim, N. Priyantha, D.T.B. Tennakoon, Sorption characteristics of peat of Brunei Darussalam III: equilibrium and kinetics studies on adsorption of crystal violet (CV), Int. J. Earth Sci. Eng., 6 (2013) 791–801.
[72] T. Zehra, N. Priyantha, L.B.L. Lim, Removal of crystal violet dye from aqueous solution using yeast-treated peat as adsorbent: thermodynamics, kinetics, and equilibrium studies, Environ. Earth Sci., 75 (2016) 1–15.
[73] S.K. Brar, N. Wangoo, R.K. Sharma, Enhanced and selective adsorption of cationic dyes using novel bio-compatible self-assembled peptide fibrils, J. Environ. Manage., 2551 (2020), doi: 10.1016/j.jenvman.2019.109804.
[74] X. Yuan, F. Zhou, R. Man, J. Huang, Dendritic post-cross-linked resin for the adsorption of crystal violet from aqueous solution, J. Chem. Thermodyn., 130 (2019) 235–242.
[75] L.B.L. Lim, A. Usman, M.H. Hassan, N.A.H.M. Zaidi, Tropical wild fern (*Diplazium esculentum*) as a new and effective low-cost adsorbent for removal of toxic crystal violet dye, J. Taibah Univ. Sci., 14 (2020) 621–627.
[76] M. Ishaq, F. Javed, I. Amad, H. Ullah, F. Hadi, S. Sultan, Adsorption of crystal violet dye from aqueous solutions onto low-cost untreated and NaOH treated almond shell, Iran, J. Chem. Chem. Eng., 35 (2016) 97–106.
[77] M. Vakili, S. Deng, G. Cagnetta, W. Wang, P. Meng, D. Liu, G. Yu, Regeneration of chitosan-based adsorbents used in heavy metal adsorption: a review, Sep. Purif. Technol., 224 (2019) 373–387.
[78] M.K. Dahri, L.B.L. Lim, M.R.R. Kooh, C.M. Chan, Adsorption of brilliant green from aqueous solution by unmodified and chemically modified tarap (*Artocarpus odoratissimus*) peel, Int. J. Environ. Sci. Technol., 14 (2017) 2683–2694.
[79] A.H. Jawad, R. Razuan, J.N. Appaturi, L.D. Wilson, Adsorption and mechanism study for methylene blue dye removal with carbonized watermelon (*Citrullus lanatus*) rind prepared via one-step liquid phase H_2SO_4 activation, Surf. Interfaces, 16 (2019) 76–84.
[80] L.B.L. Lim, N. Priyantha, C.M. Chan, D. Matassan, H.I. Chieng, M.R.R. Kooh, Adsorption behavior of methyl violet 2B using duckweed: equilibrium and kinetics studies, Arabian J. Sci. Eng., 39 (2014) 6757–6765.
[81] H. Shayesteh, A. Rahbar-Kelishami, R. Norouzbeigi, Evaluation of natural and cationic surfactant modified pumice for congo red removal in batch mode: kinetic, equilibrium, and thermodynamic studies, J. Mol. Liq., 221 (2016) 1–11.
[82] M.R.R. Kooh, M.K. Dahri, L.B.L. Lim, The removal of rhodamine B dye from aqueous solution using *Casuarina equisetifolia* needles as adsorbent, Cogent Environ. Sci., 2 (2016) 1–14.